

HIGHLIGHTS

2023

EDITO

HIGHLIGHTS 2023 INSTITUT NÉEL

February 2024
Grenoble, France

The year 2023 was a very busy one for the Institut Néel, rich in successes for the laboratory's staff, in terms of recruitment, promotions and awards, as well as events such as the inauguration of our brand-new transmission electron microscope.

Once again this year, the laboratory's teams, divisions and departments have produced some very fine results and achievements, a selection of which you will find in the following pages.

These articles illustrate the dynamism of our laboratory, and the important place it occupies in the world of research, from the local level to the international stage. They also highlight the diversity of our research themes, from the synthesis of materials to the study of their properties, from vortex dynamics to neurons and quantum systems and devices.

I would like to thank the editors, all the reviewers and Claudine Lacroix, who coordinated this edition of the Institut Néel Highlights 2023, and wish you a very pleasant reading.



© Institut Néel/CNRS - Cellule communication 2024

© Photo vuedici.org

MANAGEMENT TEAM

Unit director: *Laurence MAGAUD*

MCBT department director: *Virginie SIMONET*

PLUM department director: *Jean-Philippe POIZAT*

QUEST department director: *Jan VOGEL*

Technical director: *Nathalie BOUDET*

DIRECTOR OF PUBLICATION

Laurence Magaud

EDITORS

Claudine Lacroix, Jan Vogel

PRODUCTION MANAGERS

Nathalie Bourgeat-Lami, Florence Fernandez

LAYOUT

Florence Fernandez

PRINTING

Cyberprint

January 2024



CONTENTS

A single-electron spin qubit in an industrial transistor	5
Growth of high-quality $R\text{Te}_3$ single crystals for charge density wave tuning	6
Single layers of a two-dimensional material rotating and re-structuring	8
Dihydrogen snow dance along quantum vortex lines	10
The quantum state of $\text{Tb}_2\text{Ti}_2\text{O}_7$: beyond spin degrees of freedom	12
Imaging electric fields at nanometer length scales	14
Quantum processes can be more “non-causal” than previously thought	16
The identity crisis of individual charges in an artificial molecule	18
On the hunt for defects in $\beta\text{-Ga}_2\text{O}_3$ devices	20
Looking at magnetic textures in 3D	22
Exploring the Brain’s Wonders: graphene meets microfluidics for smarter neuroscience	24
Hybrid perovskites: opportunities and challenges for medical imaging	26
Amorphous topological states: a disordered playground for new phenomena	28
Efficient, non-toxic microwatt thermoelectric Microgenerators	30
New Transmission Electronic Microscope	32

KEY FIGURES

3 departments	35 soutenances de doctorat, 60 stages de Master par an
16 teams & 17 technical groups & services	6 start-ups, around 40 active patents, 25 operating licenses, several dozen industrial partnerships
460 researchers, teacher-researchers, engineers, technicians and administrative staff, including 160 non-permanent	60 awards since 2007
40 nationalities	40 M€ consolidated budget (including approximately €12 million in own resources)
22000 m² surface	25 thesis defenses 110 seminars
400 publications per year and over 14,000 citations per year	

EVENTS



Lycée Argouges students inaugurate their frescoes at the Institut Néel. They were created in collaboration with the laboratory and two graphic artists.



After a courtesy visit to the President of Grenoble Alpes University and in the context of the strategic partnership with the University of Tsukuba (Japan), the Mayor of Tsukuba (Dr. Igarashi) visited the Institut Néel.

DELEGATIONS @ NÉEL

Netherlands, Tsukuba, Sherbrooke, University of Norway NTNU, University of Taiwan, QuantAlps Federation, CNRS@CREATE

INAUGURATION TEM



From left to right: M. Fraisse (Délégue Régionale Alpes, CNRS), A. Schuhl (Directeur général délégué à la science du CNRS), L. Piquier (Vice-président senior, excellence opérationnelle et directeur technique, Constellium), S. Sisaid (sous-préfet à la relance), C. Staron (Vice-présidente déléguée à l'enseignement supérieur, à la recherche et à l'innovation de la Région Auvergne-Rhône-Alpes), L. Magaud (Directrice d'Unité Institut Néel). See page 32.

A SINGLE-ELECTRON SPIN QUBIT IN AN INDUSTRIAL TRANSISTOR

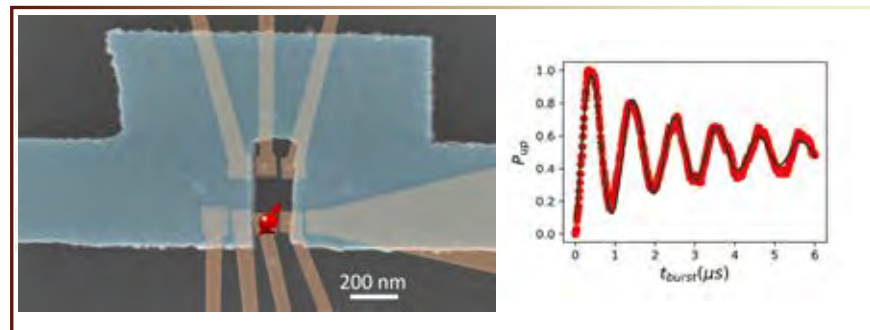
To fully realize the potential of quantum information, millions of interconnected qubits are required. The use of Complementary Metal-Oxide-Semiconductor (CMOS) technology, which has enabled the integration of billions of transistors in classical computers, seems to be a natural solution. Semiconductor spin qubits exhibit high coherence times and can be integrated using CMOS technology, making them an ideal candidate for reliable and scalable manufacturing.

This work focuses on the fabrication and characterization of intermediate solutions to transition from academic qubit fabrication to qubits fully compliant with industrial CMOS standards. Specifically, our research has centered on studying a single-electron spin qubit in a CMOS device using a micro-magnet integrated into the manufacturing process. This micromagnet generates an inhomogeneous field in which the electron moves. When this movement occurs at a specific frequency, the electron's spin, behaving like a nanomagnet, starts to rotate. The same principles applied in magnetic resonance measurements, such as spin echoes, are implemented here which has allowed us to study the effect of its environment on decoherence, such as charge or nuclear spin fluctuations, and the presence of excited states related to the valley structure of sili-

con. The results indicate that the system's coherence is limited at low-frequency by residual nuclear spins in the natural silicon channel and at high frequency by charge noise.

The work presented here provides the first experimental evidence of coherent manipulation of an electron in a structure compatible with microelectronics. Subsequently, the introduction of isotopically pure silicon is considered to significantly enhance coherence properties.

Figure 1



Captions

Figure 1: Scanning Electron Micrograph of the Micro-Magnet Deposited on the CMOS Device.

A single electron is trapped within the CMOS device, and its spin is manipulated via electric dipole spin resonance, induced by the gradient field created by the micro-magnet. The oscillations in the right figure depict this coherent manipulation, enabling the creation of an arbitrary superposition of states of the qubit.

FURTHER READING



Electrical manipulation of a single electron spin in CMOS with micromagnet and spin-valley coupling



B. Klemt*, V. Elhomsy* and al.

NPJ Quantum Information, volume 9, 107 (2023) – arXiv:2303.04960



Matias Urdampilleta, matias.urdampilleta@neel.cnrs.fr

PhDs

Bernard Klemt & Victor Elhomsy

GROWTH OF HIGH-QUALITY $R\text{Te}_3$ SINGLE CRYSTALS FOR CHARGE DENSITY WAVE TUNING

Low dimensional materials with 2D van der Waals interactions can host exciting electronic properties with strong anisotropic behavior. We present here the growth of high-quality single crystals of the rare earth tritelluride $R\text{Te}_3$ exhibiting a charge density wave (CDW) at room temperature and antiferromagnetic order at low temperature.

Single crystals of $R\text{Te}_3$ ($R = \text{Gd}, \text{Tb}, \text{Ho}, \text{Er}$) were prepared in a glove box from elements of high chemical purity. Self-flux method was used as the compounds melt non congruently, with the flux composition and the reaction temperature determined precisely from the different R-Te phase diagrams. Typically the R and Te precursors with the molar composition $R\text{Te}_3:\text{Te}$ 2:98 are sealed in a quartz tube under vacuum, heated at 750–800°C for 48 hours and slowly cooled at 2°C/h to 450°C. Single crystals are extracted from the Te flux by centrifugation. This results in shiny plates of metallic gold color ranging from 2 mm² to 1 cm².

Several R-Te phases are present in the rich Te region of the phase diagrams. Their crystal structures are closely related to the $R\text{Te}_3$ phase, with different stackings of the same motifs (Fig. 1). Both $R\text{Te}_2$ and $R_2\text{Te}_5$ host similar physical properties (2D magnetism,

CDW). Control of the reaction parameters is therefore crucial to the quality of the crystal and to the subsequent physics studies performed with them.

$R\text{Te}_3$ compounds crystallize in the orthorhombic $Cmcm$ space group. The structure consists of a corrugated RTe slab sandwiched by two nearly square-planar Te sheets stacked up along the b axis through van der Waals forces between adjacent Te layers. All these compounds exhibit a transition to a state with an incommensurate unidirectional CDW with a wave vector Q_1 (0, 0, $\sim 2/7$ c*) at the transition temperature T_{CDW1} higher than 250 K. For heavy R elements (Dy, Ho, Er, Tm), a second transition occurs at lower temperature to a state with an independent orthogonal CDW with the wave vector Q_2 ($\sim 2/7$ a*, 0, 0). Fig. 2 shows the breaking of the conductivity isotropy along a and c axis for ErTe_3 below T_{CDW1} .

At low temperature a magnetic order originates from the highly localized magnetic moment of R^{3+} in the RTe slab. For TbTe_3 three successive magnetic transitions occur, antiferromagnetic at $T_{\text{N1}} = 6.7$ K and $T_{\text{N2}} = 5.7$ K, and one at $T_{\text{N3}} = 5.4$ K to an incommensurate modulation intertwined with the CDW modulation (Fig. 3).

Slight deformation of the crystal structure of TbTe_3 can have a dramatic influence on the elec-

tronic order that is stabilized. In particular, it has been shown that the CDW developed along the c axis in the pristine state ($c/a < 1$) switches to an orientation along a when $c/a > 1$. This is achieved by performing true biaxial mechanical deformation of a TbTe_3 sample from 250 to 375 K, and by measuring both structural and electronic parameters with x-ray diffraction and transport measurements. We show that this switching transition is driven by the structural parameter c/a , and that the transition occurs for $a = c$, with a coexistence region for $0.9985 < a/c < 1.002$.

This work was performed within the international ANR Bisceps framework, in collaboration with the Kotelnikov Institute of Moscow, the LPS in Orsay and the Institut Pprime in Poitiers. It relied on the synthesis of high-quality single crystals by the Institut Néel crystal growth team.

We recently made progress in the growth of these crystals, increasing their thickness up to 3 mm. The new crystals have suitable sizes for neutron experiments and the magnetic behavior of HoTe_3 is currently studied.

Figure 1

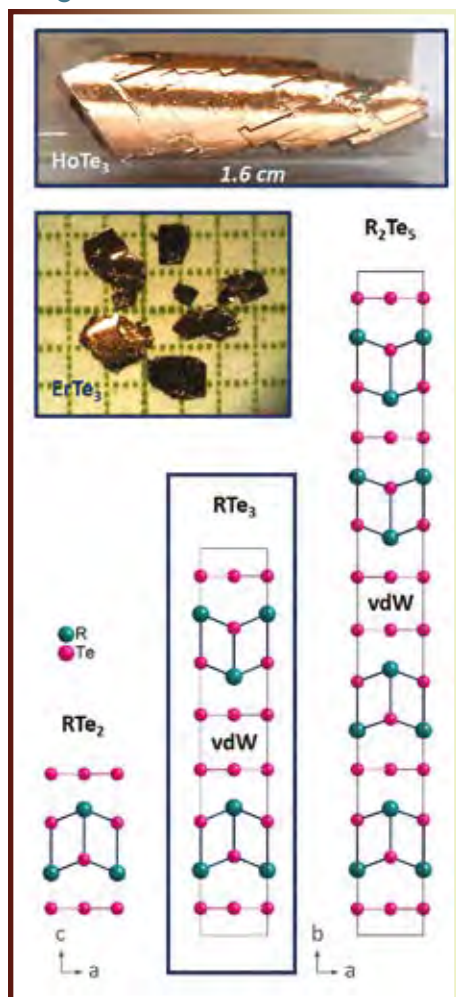


Figure 2

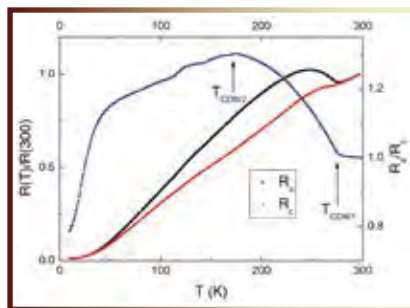
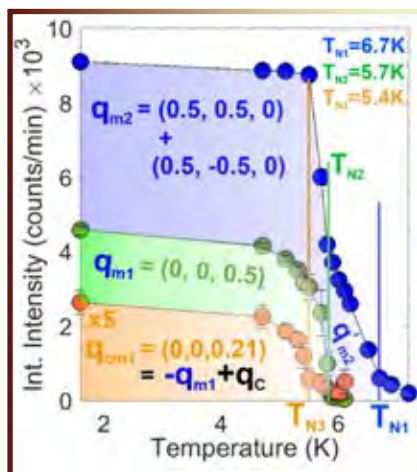


Figure 3



Captions

Figure 1: Pictures of various RTe₃ single crystals. Comparison of the RTe₃ orthorhombic Cmc crystal structure with RTe₂ P4/nmm and R₂Te₅ Cmc structures.

Figure 2: Temperature dependence of normalized resistance $R(T)/R(300K)$ and conductivity anisotropy $R_a(T)/R_c(T)$ along a and c in ErTe₃.

Figure 3: Temperature dependence of the magnetic peak intensities measured with neutron diffraction showing the three consecutive magnetic transitions in TbTe₃. The magnetic order is commensurate antiferromagnetic below T_{N1} and T_{N2} , and switches to an incommensurate modulation below T_{N3} .

FURTHER READING



Strongly coupled charge, orbital and spin order in TbTe₃



S. Chillal, E. Schierle, E. Weschke, F. Yokaichiya, J.-U. Hoffmann, O.S. Volkova, A.N. Vasiliev, A.A. Sinchenko, P. Lejay, A. Hadj-Azzem, P. Monceau & B. Lake

Phys. Rev. B 102, 211110(R), 2020



Charge Density Waves Tuned by Crystal Symmetry



A. Gallo-Frantz, V.L.R. Jacques, A.A. Sinchenko, D. Ghoneim, L. Ortega, D. Le Bolloc'h, P. Godard, P.-O. Renault, P. Grigoriev, A. Hadj-Azzem, J.E. Lorenzo, P. Monceau, D. Thaiudière, E. Bellec

hal-04251892, 2023



Abdellali Hadj-Azzem, abdellali.hadj-azzem@neel.cnrs.fr

Elise Pachoud, elise.pachoud@neel.cnrs.fr

Pierre Monceau, pierre.monceau@neel.cnrs.fr

SINGLE LAYERS OF A TWO-DIMENSIONAL MATERIAL ROTATING AND RE-STRUCTURING

Tantalum disulphide can be grown in the form of a single layer (only three-atom-thick) on a substrate. This material expectedly hosts a quantum fluid of electrons called a charge density wave. Like other two-dimensional materials, it forms a moiré, i.e. a nanoscale pattern, with its substrate. We found that intercalating atomic layers of alkali atoms between the substrate and the material gives freedom for the latter to rotate, and accordingly to form new kinds of nanoscale patterns. One of them might be a so-far unreported charge density wave.

Tantalum disulphide (TaS_2) is known for decades as a thick, multilayer material. Its electrons can significantly interact with each other, resulting in macroscopic quantum phases – a superconducting state and a so-called charge density wave. With the advent of two-dimensional materials, i.e. few-atom-thick materials such as single layers of transition metal dichalcogenides like TaS_2 , the exciting question whether these quantum phases survive or can be manipulated has been addressed. So far, the answer is not conclusive, with reports of charge density waves quenched, or on the contrary stabilised by the interaction with a substrate.

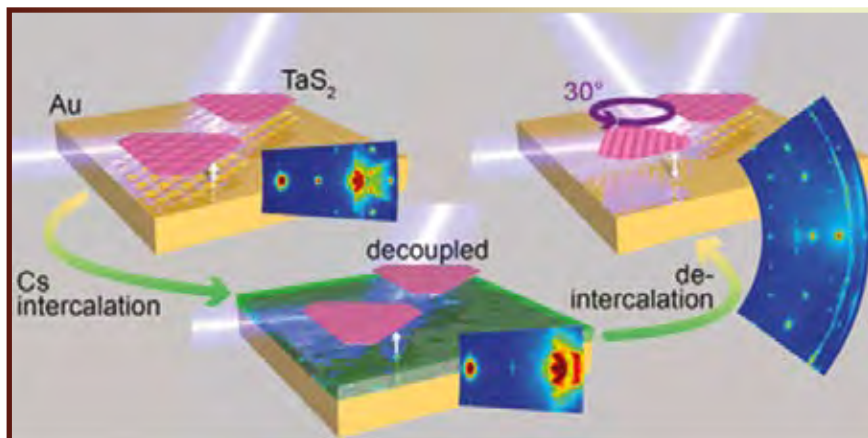
Within a consortium lead by IRIG/MEM, strongly involving three groups at Institut Néel (EpiCM, CRG, Quan2um), we have:

- developed the epitaxial growth, with atomic beam deposition under a reactive atmosphere (H_2S) under ultrahigh vacuum, of single-layer TaS_2 on a $\text{Au}(111)$ substrate;
- introduced a new route to the decoupling of the TaS_2 from its substrate, exploiting the thermally-activated intercalation of atomic layers of cesium;
- characterised the structure of TaS_2 , before, during, and after intercalation, with a high resolution and in situ, using high-resolution scanning tunneling microscopy at Institut Néel and surface X-ray diffraction at the INS2 instrument installed at the BM32 CRG beamline of the ESRF.

The high-resolution structural analysis was particularly rich, revealing a wealth of fine structural and compositional changes of the two-dimensional layer when the temperature changes and the intercalation/de-intercalation occur (Fig. 1). It was for instance possible to detect changes in the atomic structure of the moiré (Fig. 2), changing from a first-order to a second-order (larger scale) periodicity or even fully vanishing upon intercalation.

Even more strikingly, the vanishing of the moiré, signaling a strongly weakened interaction between the TaS_2 and $\text{Au}(111)$, was accompanied with a rotation of the TaS_2 layer, by 30° . In this rotated state, after de-intercalation the layer adopts two new superstructures (i.e. other than the initial moiré). One of them, a commensurate structure between the lattices of TaS_2 and Au , features perfect periodic atomic coincidence, and is “simply” a rotated moiré. The other superstructure is incommensurate, and more puzzling for this reason. It corresponds to a weak interaction between TaS_2 and Au , and it might be related to the charge density wave that is otherwise absent in TaS_2 on $\text{Au}(111)$.

Figure 1

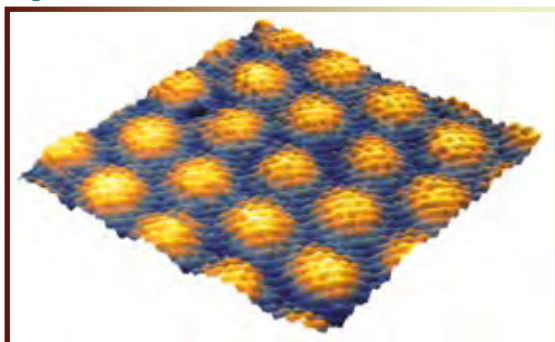


Captions

Figure 1: Three-dimensional cartoons, together with maps of the reciprocal space, showing the structural changes in a two-dimensional TaS_2 grown on a $\text{Au}(111)$ substrate, during (de) intercalation of an atomic layer of Cs atoms.

Figure 2: Atomic-resolution scanning tunneling microscopy image of two-dimensional TaS_2 grown on $\text{Au}(111)$, revealing the 2.3 nm period of the moiré. This pattern results from the slight lattice mismatch between TaS_2 and $\text{Au}(111)$, hence the spatially-varying relative atomic stacking.

Figure 2



FURTHER READING

 **Superstructures, Commensurations, and Rotation of Single-Layer TaS_2 on $\text{Au}(111)$ Induced by Cs Intercalation/Deintercalation**

 X. Weng, P. David, V. Guisset, L. Martinelli, O. Geaymond, J. Coraux & G. Renaud
ACS Nano, 17, 5459 (2023)

 **Philippe David**, philippe.david@neel.cnrs.fr
Valérie Guisset, valerie.guisset@neel.cnrs.fr

DIHYDROGEN SNOW DANCE ALONG QUANTUM VORTEX LINES

By visualizing dihydrogen particles, we can now follow a whole network of quantum vortices in rotating Helium-4, with vortex core of the size of an atom. Observation of the dynamics of these vortices establishes a reference experimental regime for consolidating descriptions of all quantum fluids.

The study of the dynamics of quantum vortices in the superfluid phase of liquid Helium-4, known as "He II", holds great promise to refine theoretical descriptions of quantum fluids. Bose-Einstein condensates, neutron stars, and even superconductors exhibit quantum vortices, whose interactions are crucial in energy dissipation in these systems. The properties of the velocity field around the core of these objects are quantified, and in He II, this core is as thin as a helium atom...

They have been observed experimentally by indirect means, such as the damping of second sound waves or via their interaction with electrons. In addition, over the last twenty years, seeding cryogenic flows with solid particles has proved to be a very effective method to study these vortices. However, in these pioneering observations, on the one hand, experimental stability, initial conditions, stationarity,

and reproducibility were poorly controlled. On the other hand, the investigations assumed two-dimensional dynamics in systems where they were intrinsically 3D.

Our experimental apparatus (Fig. 1) allows us to generate quantum vortex lattices with relative ease and controlled reproducibility. With complete control of pressure, temperature, particle injection parameters, and rotational speed, various conditions can be explored to further our understanding of these quantum objects. Our first endeavor has proven that solid dihydrogen particles are good quantum vortex tracers. Indeed, in simple stationary rotation conditions, the dihydrogen snow aggregates along lines that quantitatively follow Feynman's rule of quantum vortex spacing. With optical cameras, we could then directly visualize a slice of an Abrikosov lattice aligned with the rotation axis, as found in Bose-Einstein condensates or superconductors.

Critically, this stationary rotation and seeding of tracers allow us to build a reproducible, well-defined, well-controlled initial condition for further experiments. As an example, introducing an alternating heat flux at the bottom of the experiment and along the axis of rotation induces waves that propagate along the vor-

tices (Fig. 2). At low amplitudes, the nature of those oscillations reveals the interactions at play in the vortex lattice. In contrast, at large amplitudes, they destroy the lattice and generate a plethora of vortex reconnections, which have only been observed as singular events up to now. This succession of regimes defines a controlled path towards quantum turbulence in rotating He II and a reference experiment for consolidating descriptions of quantum fluids.

Figure 1

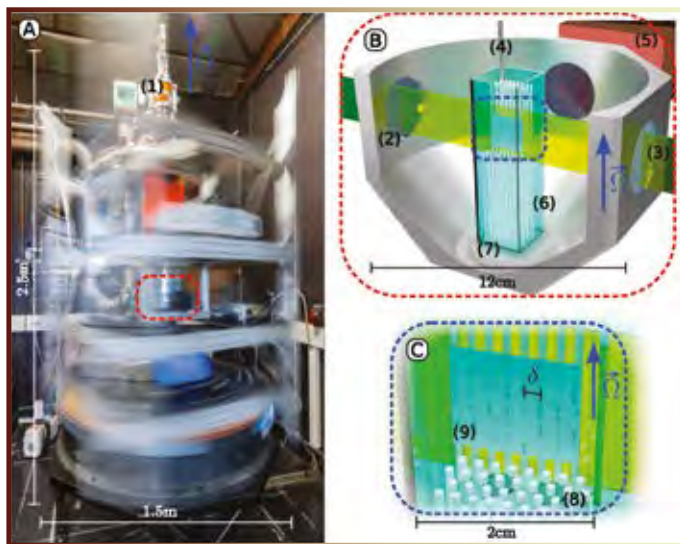
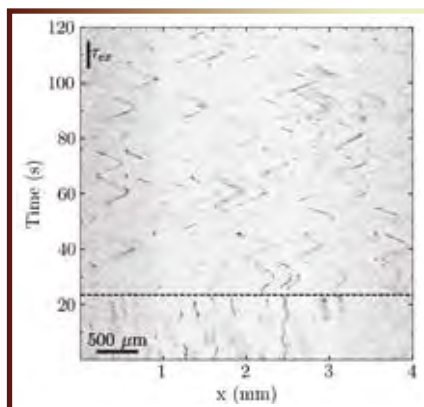


Figure 2



FURTHER READING



Direct visualization of the quantum vortex lattice structure, oscillations, and destabilization in rotating ^4He



C. Peretti, J. Vessaire, É. Durozoy & M. Gibert

Science Advances. <https://doi.org/adh2899>

De la neige d'hydrogène pour voir les tourbillons quantiques

<https://www.inp.cnrs.fr/fr/cnrsinfo/de-la-neige-dhydrogene-pour-voir-les-tourbillons-quantiques>



Jeremy Vessaire, jeremy.vessaire@neel.cnrs.fr

Gregory Garde, gregory.garde@neel.cnrs.fr

Mathieu Gibert, mathieu.gibert@neel.cnrs.fr

PhD students

Charles Peretti & Émeric Durozoy

Captions

Figure 1: Rotating cryostat and explanation of the measurement.

Image A is a photo of the rotating cryostat. Diagram B shows a zoomed-in slice of the final layer of the experimental cell, which is filled with Helium during the experiments. This is an elongated square cupola with multiple optical ports (2) (transparent to the visible light spectrum) at different angles. These allow a laser sheet (3) to illuminate a vertical slice of the experimental volume. This laser sheet is used to illuminate solid particles of dihydrogen. In the canonical case of constant rotation, a network of vortices forms inside the channel. Diagram C is enlarged to show the hexagonal network of quantum vortices (8). The white vertical cylinders are a representation of the vortex cores. For ease of reading, they are not to scale and are cut horizontally. The experimental photograph (9) is an order of magnitude larger than the real thing (here, the experimental image is about 1.4 mm wide, the axes equal, and the channel is 2 cm wide).

Figure 2: Space-time visualization of wave propagation along quantum vortices.

Space-time representation of a single horizontal line of pixels in an experimental movie at angular velocity $\Omega = 5.236 \times 10^{-1} \text{ rad s}^{-1}$ (5 rpm). Scale bars, 500 μm (horizontal) and τ_{ex} 10 s (vertical). The horizontal dotted line indicates the time t_0 after which the heater is activated with a periodic positive square function of period τ_{ex} and heating power 3.6 mW over a period (9 W m^{-2}). Although periodic horizontal movement exists before t_0 , the heat injection after t_0 generates ample periodic horizontal motion coming from the wave propagation along the vortices.

THE QUANTUM STATE OF $Tb_2Ti_2O_7$: BEYOND SPIN DEGREES OF FREEDOM

Spin liquids are exotic states that can occur in magnetic materials where strong exchange interactions between the magnetic moments cannot stabilize a long-range magnetic order. One of the possible origins is geometric frustration, popularly exemplified by a network of corner-sharing tetrahedra of spins (in the so-called pyrochlore lattice) with nearest-neighbor antiferromagnetic exchange interactions. Here we show the use of high-resolution THz spectroscopy to shed light on the origin of the spin liquid state in the pyrochlore oxide $Tb_2Ti_2O_7$, which has been elusive for more than 20 years.

$Tb_2Ti_2O_7$ is a pyrochlore oxide where the magnetic carriers are Tb^{3+} ions forming a network of corner-sharing tetrahedra (see Fig. 1) with antiferromagnetic exchange interactions. The strong crystalline electric field induced by the oxygen ions surrounding the Tb and the strong orbital contribution to the Tb magnetic moment lead the magnetic moments to point inward or outward from the center of each tetrahedron. With anti-ferromagnetic exchange interactions, one would expect stabilization of a magnetic order where the magnetic moments point either all towards the interior or all to the exterior of each tetrahedron. This is not the case, down to temperatures as low as 70mK, and the reason for

this has for long remained puzzling. It has been suggested that quantum effects implying more complex ingredients play a role: the coupling of the spins to the lattice and the competition with quadrupolar degrees of freedom.

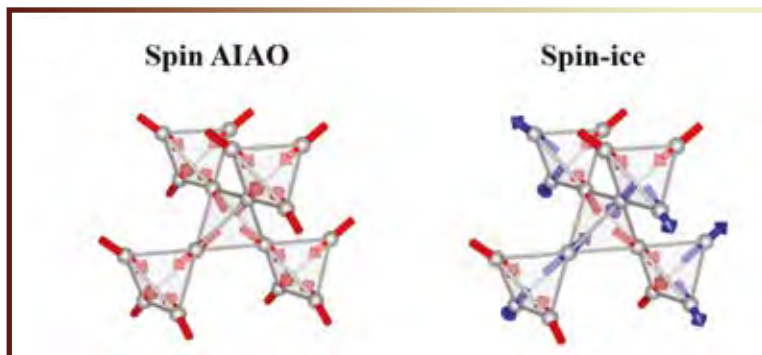
Quadrupolar degrees of freedom exist as soon as the magnetic moment exhibits a quantum angular momentum $J \geq 1$, in the presence of complex electronic densities with low symmetries. Generally, they prove irrelevant to dipole magnetism and can therefore be ignored. However, in some instances their effects can have a large influence on magnetic order as we have revealed in $Tb_2Ti_2O_7$.

A detailed experimental investigation of the electronic state of Tb^{3+} evidenced intriguing features. Using high resolution THz spectroscopy, we have been able to probe the low energy electronic spectrum of Tb^{3+} in $Tb_2Ti_2O_7$. Instead of the expected single transition, we observe a fine structure with 4 transitions revealing that the ground state of Tb^{3+} ions in this compound is not the ground state expected in the perfect pyrochlore because it interacts with the surrounding lattice, but without inducing any static distortion: it is a dynamical effect. This implies that the description of $Tb_2Ti_2O_7$ should not only contain spin degrees of freedom but also their couplings to other degrees of freedom, associated to the lattice. These couplings can

be described using quadrupolar operators that affect the quadrupolar electronic density of states of Tb^{3+} ions. A schematic view of their arrangement in this oxide is displayed in Fig. 2. Our THz measurements have then revealed indirectly the effects of the quadrupoles.

We subsequently observed that the effects of the quadrupoles are extremely sensitive to small amounts of disorder in the system: a small off-stoichiometry $Tb_{2+x}Ti_{2-x}O_{7+d}$ with $x = \pm 0.003$ is able to change the strength of the coupling mechanism. We understand this by the presence of direct quadrupolar couplings that compete with the lattice mediated couplings. We therefore show that frustration mechanisms may exist, in a more general way than the already known spin dipolar frustration, with higher order multipoles.

Figure 1



Captions

The pyrochlore lattice of corner sharing tetrahedra

Figure 1: Two possible spin configurations when all spins point inward or outward with respect to the center of each tetrahedron (Spin all in – all out AIAO) or two of them point inward, two outward (the so-called Spin-ice). The former is expected for $Tb_2Ti_2O_7$, but not observed.

Figure 2

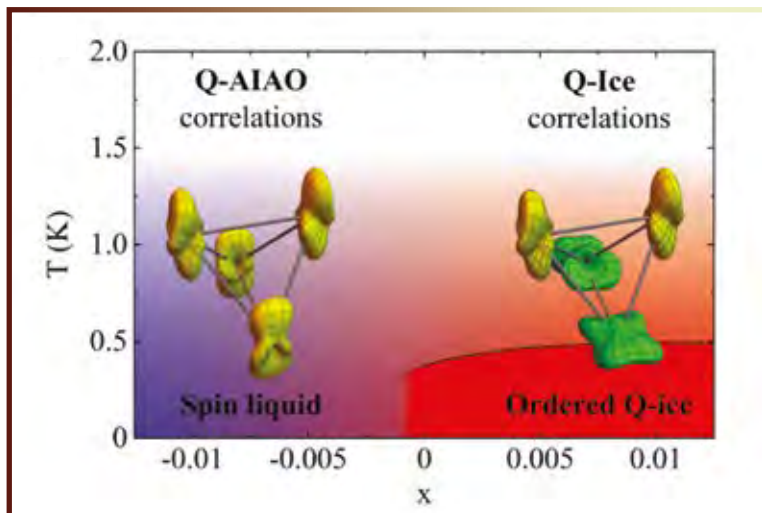


Figure 2: Similarly, for the quadrupole parts, all in –all out configuration (Q-AIAO) may exist as well as two in-two out (Q-ice). The two configurations can be stabilized in $Tb_{2+x}Ti_{2-x}O_{7+d}$ depending on the off-stoichiometry x.

FURTHER READING



Magneto-optical investigation of quadrupolar spin lattice effects in magnetically frustrated $Tb_2Ti_2O_7$



K. Amelin, Y. Alexanian, U. Nagel, T. R    m, J. Robert, J. Debray, V. Simonet, C. Decorse, Z. Wang, R. Ballou, E. Constable & S. de Brion

Phys. Rev. B 102, 134428 (2020)



Vibronic collapse of ordered quadrupolar ice in the pyrochlore magnet $Tb_{2+x}Ti_{2-x}O_{7+y}$



Y. Alexanian, J. Robert, V. Simonet, B. Langerome, J.-B. Brubach, P. Roy, C. Decorse, E. Lhotel, E. Constable, R. Ballou & S. de Brion

Phys. Rev. B 107, 224404 (2023)



Sophie de Brion, sophie.debrion@neel.cnrs.fr

PhD student

Yann Alexanian, now at Universit   de Gen  ve

Semiconductor p-n junctions are basic building blocks for devices like transistors, solar cells, avalanche photodetectors or light emitting diodes. To implement the junction, the electrical properties of semiconducting materials are engineered by adding just very few (less than 1%!) dopant atoms that donate or accept an electron to the conduction or from the valence band, respectively. In this way, the density of mobile charges in the semiconducting material can be tuned over several orders of magnitude.

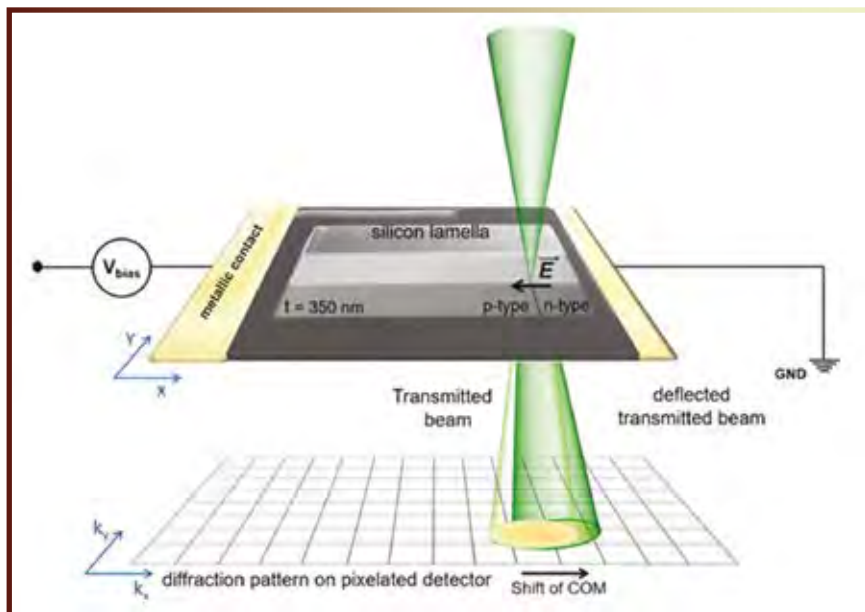
It is very well known that a transition from a region with one type of dopant (donors or acceptors) to the other kind will generate a depletion region with almost no free charges but an electric field, a so-called p-n junction, giving rise to interesting properties such as rectifying current voltage characteristics and potentially light emission, for example in light emitting diodes. However, challenges remain to control and measure the electrically active doping levels in semiconducting materials with nm precision. One aspect of a p-n junction is its abruptness: how fast the transition from one dopant atom to the other is made. This property influences the electric field strength present at the junction and thereby the characteristics of a device made from the junction.

Transmission Electron Microscopy (TEM) is interesting with regards to dopant characterization due to its high spatial resolution from few nm to atomic spatial resolution, as well as the penetration through the sample (hence transmission). When an electron probe traverses a region in the sample containing an electric field in the plane of the sample, the electrons are deflected by the field. This beam deflection can be measured very precisely if an image of the transmitted probe is made at each scan location of the probe on the sample, while scanning the sample point by point with a nm sized probe and making nm sized scanning steps. This technique is referred to as 4D-STEM, see Fig. 1. Because the technique is sensitive only to the projected electric field, only electrically active dopants will be contributing to the signal. However, material contrast does contribute to the signal, but is invariable with applied bias.

In this work, in collaboration with colleagues at CEA Grenoble in IRIG and LETI at the Nano Characterization platform (PFNC), we have performed such experiments on a p-n junction in silicon, using a very high quality and fast direct electron detector, as well as electrical contacts to the p-n junction thin film sample. The contacts to the sample allow measuring the internal field as a function of applied external bias voltage, see Fig. 2. From

the measured electric field map at each applied bias voltage, we can calculate the charge density map. We have then compared the measured electrical properties (electric field and charge density) with calculated ones assuming either a perfectly abrupt transition from p to n dopants, or a linearly graded one. Our analysis showed that the junction under study could be rather well approximated by a linear graded junction. This work shows that quantitative electrical information at nm length scale is possible by 4D-STEM and that this powerful technique allows to probe the doping profile in semiconductors determining their electrical properties. This work was carried out at the TEM in PFNC in CEA. The installation of two new state of the art TEM's both at Institut Néel and at the PFNC will certainly boost this activity and will allow obtaining even better-quality electrical field maps on semiconducting samples, further improving signal to noise as well as spatial resolution.

Figure 1

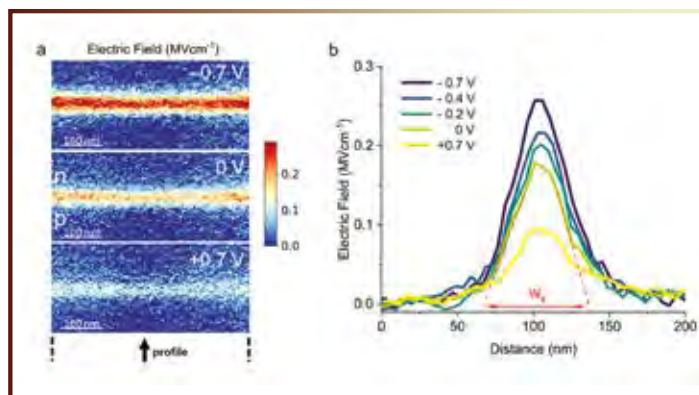


Captions

Figure 1: Concept of a 4D-STEM experiment performed in a silicon p-n junction with electrical contacts.

Figure 2: (a) In situ biased 4D-STEM electric field maps of the silicon p-n junction for different applied bias voltage. (b) Profiles of the electric field obtained from (a) by integration along the entire map length, as indicated in (a). The measured depletion length for zero bias is indicated by W_d .

Figure 2



FURTHER READING



Assessment of Active Dopants and p-n Junction Abruptness Using In Situ Biased 4D-STEM



B.C. da Silva, Z.S. Momtaz, E. Monroy, H. Okuno, J.L. Rouvière, D. Cooper & M.I. den Hertog
Nano Letters 22,23, 9544–9550 (2022) – <https://dx.doi.org/10.1021/acs.nanolett.2c03684>



The influence of illumination conditions in the measurement of built-in electric field at p-n junctions by 4D-STEM



B.C. da Silva, Z.S. Momtaz, L. Bruas, J.L. Rouvière, H. Okuno, D. Cooper & M.I. den Hertog
Applied Physics Letters 121, 123503 (2022) – <https://doi.org/10.1063/5.0104861>



Martien den Hertog, martien.den-hertog@neel.cnrs.fr
 Jean Luc Rouviere (IRIG), jean-luc.rouviere@cea.fr
 David Cooper (LETI), david.cooper@cea.fr

Post-Doc

Bruno Cesar da Silva

QUANTUM PROCESSES CAN BE MORE “NON-CAUSAL” THAN PREVIOUSLY THOUGHT

Much like how certain properties can fail to be well-defined in the quantum world—e.g., a cat can be in a superposition of being “both alive and dead” simultaneously—it has been realised in the past 15 years that the causal relations between quantum events could also be indefinite—e.g., two events *A* and *B* can be arranged in a superposition of “both *A* causes *B*, and *B* causes *A*”. We found recently that certain quantum processes, which can be realised in the lab, can manifest a very strong form of such “non-causality”, resulting in the violation of what are known as “causal inequalities”—the causal counterpart to Bell inequalities.

Causality is a fundamental concept that underpins our understanding of the physical world. We typically conceive of events unfolding in a well-defined causal order, with past events being able to influence future events, but not vice versa.

In the past 15 years, researchers started to investigate what happened to the concept of causality when one enters the quantum world, and whether this classical notion of well-defined causal relations remains intact in the quantum realm. It was soon realised that certain quantum processes could exhibit some peculiar form of “causal indefi-

niteness”. The paradigmatic example of this is the so-called “quantum switch” (see Fig. 1): a process in which the causal order between two operations *A* and *B* is controlled by the state of a quantum system: if that “control qubit” is in the state $|0\rangle^c$ then *A* is applied before *B* (on a separate “target system”), and vice versa for the control state $|1\rangle^c$; if the control qubit is prepared in a superposition $\frac{|0\rangle^c + |1\rangle^c}{\sqrt{2}}$, then a coherent superposition of the two causal orders arises.

One can draw an analogy between such “noncausality” and the better-known “nonlocality” of quantum theory. Entanglement (also called quantum “nonseparability”) is at the heart of quantum nonlocality; analogously, we define the notion of “causal nonseparability” to characterize processes with indefinite causal orders. The most extreme form of nonlocality is exhibited through the famous violation of Bell inequalities; similarly, certain causally indefinite processes are predicted to violate so-called “causal inequalities”.

There is a caveat here, however: the quantum switch above cannot violate such causal inequalities. It has in fact remained an open question, whether it was possible to physically realise, in a laboratory setting, a process that would exhibit this extreme form of noncausality. And while many believed this to be impossible, we

have recently provided a positive response to this question, exhibiting such a noncausal process.

This process takes the form of a quantum circuit, as in Fig. 2. The crucial point was to identify the operations that are applied in an indefinite causal order, and the precise systems upon which these operations act. For this we needed to consider the recently introduced notion of “time-delocalised systems”: much like quantum systems and operations can be delocalised in space (a particle can be “here and there”), they can also be delocalized in time (a system can exist, and acted upon “now and then”). Here we found a new way to delocalise the operations in time, in such a way that these operations can indeed violate causal inequalities.

That quantum phenomena can actually exhibit such strong form of causal indefiniteness further challenges our understanding of causality in the quantum domain. The full extent of its implications for our understanding of time and causality is yet to be unveiled. Beyond its significance for fundamental physics, this finding also holds promise for potential applications in information processing, that would exploit time-delocalised operations.

Figure 1

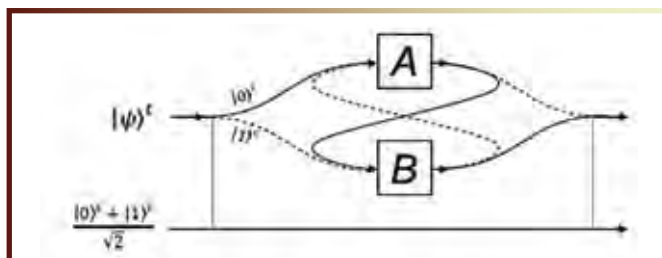
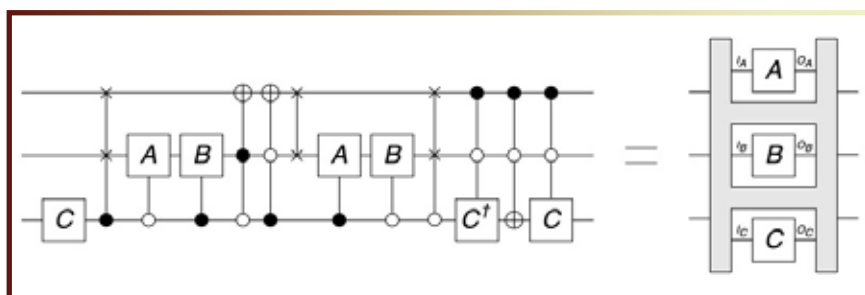


Figure 2



Captions

Figure 1: The “Quantum switch”: Depending on the state of the control system, $|0\rangle^c$ or $|1\rangle^c$, the target system—initially in the state $|\psi\rangle^t$ —undergoes either A before B (solid line trajectory) or vice-versa (dashed trajectory). For a control in a quantum superposition $\frac{|0\rangle^c + |1\rangle^c}{\sqrt{2}}$, we obtain a superposition of the two orders. Despite being “causally nonseparable”, the quantum switch cannot violate causal inequalities.

Figure 2: The left hand side represents a quantum circuit, in which quantum systems (horizontal lines, evolving from left to right) undergo a number of operations (represented by the various symbols on the lines). One can identify some subsystems I_x and O_x ($x=A, B, C$) that are “time-delocalised” in this circuit, and which define the input and output systems of the quantum operations A, B and C , as represented schematically on the right. These operations can now violate a causal inequality—demonstrating a very strong form of “causal indefiniteness”.

FURTHER READING



Existence of processes violating causal inequalities on time-delocalised subsystems



J. Wechs, C. Branciard & Ognyan Oreshkov

Nature Communications **14**, 1471 (2023) ; e-print arXiv:2201.11832



Cyril Branciard, cyril.branciard@neel.cnrs.fr

THE IDENTITY CRISIS OF INDIVIDUAL CHARGES IN AN ARTIFICIAL MOLECULE

When coupling individual quantum systems, it is possible to create more than the sum of its parts. This already holds for classical pendulums that are connected by a spring. Their characteristic motion becomes distributed across both masses and become collective excitations. A very similar concept applies to quantum world.

One example of a prototypical quantum system is a solid state qubit, which is the quantum analogue of the classical computational unit, the bit. It is therefore the building block of a quantum computer. However, no computations can be performed with just a single qubit. This shows that we require interactions between these quantum systems. Our realisations of qubits are semiconductor quantum dots, so-called artificial atoms. By bringing two of these quantum dots within 10 nanometers of each other the quantum tunnelling of charge carriers between them introduces the required interaction. To stress the resulting hybridization of the charge carrier states, these semiconductor nanostructures are called quantum dot molecules.

The key resource of quantum technology is the coherence, which describes the 'quantumness', i.e. a capability to sustain a superposition state, and distinguishes the qubit from the bit. So we can conclude that the groundwork of quantum tech-

nologies is the ability to transport coherence between qubits! To achieve that aim, ground-breaking experimental methods have emerged to manipulate individual qubits in various platforms. High-fidelity computations can nowadays be performed between superconducting qubits with the interactions mediated by microwave cavities. Coherent energy transfers between individual atoms and ions can be tailored at will and a substantial progress has been achieved in their coupling by nano-cavities and even optical fibres extending the wiring to distances on a meter scale.

In semiconductors, single electron spins in gate-controlled quantum dots are now routinely isolated and coherently displaced across mesoscopic channels to generate distant spin entanglement. In the optical domain, a cooperative super-radiant emission, between pairs of emitters embedded in photonic crystal waveguides have recently been achieved, employing colour centres in diamond and semiconductor quantum dots. The relevance of these artificial atoms in science and emerging technology has just been recognized with the Nobel Prize in Chemistry in 2023.

In spite of this supreme recognition, ascertaining coherent coupling between individual electronic excitations inside QDs, is still in its infancy. And yet, the so-called quantum dot excitons, which represent the qubit, can be

well controlled with external laser fields, permitting to carry out coherent control at sub-picosecond timescales, beyond cryogenic temperatures, even up to ambient conditions.

Because the epitaxial growth and processing of semiconductors, especially on the GaAs material platform, has been driven close to perfection, advanced nanostructures can today be merged with smart photonic devices.

Triggered by the international collaboration, we combined cutting-edge science and technology on all levels of semiconductor quantum photonics to demonstrate controlled coherent coupling between exciton qubits in a quantum dot molecule. In this device charge carriers do not remain confined in a single quantum dot, but can be hybridly shared by both artificial atoms. This classically counterintuitive phenomenon is enabled by the quantum tunnelling effect of the charge carriers.

The high-quality semiconductor nanostructures were conceived and fabricated by coordinated efforts of partners in Germany. The decisive proof for coherent coupling was revealed by performing ultrafast two-dimensional four-wave mixing (2DFWM) spectroscopy at Institut Néel in Grenoble. This advanced method allows to directly monitor the evolution of the fundamental quantum coherence in a stroboscopic way. With this approach we were able to demonstrate that the hybridization of states really

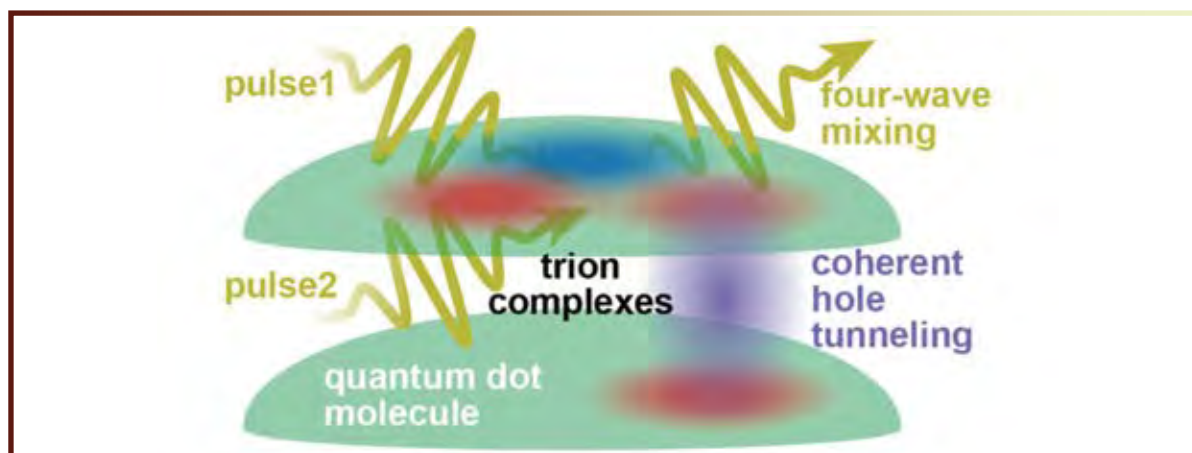
happens on a quantum level conserving the coherent properties required for future applications. The theoretical understanding and quantitative description of the spectroscopic data was provided by collaborating groups in Wrocław and Dublin. Applying this method in the past, the optical control of individual quantum dot excitons was detected and interpreted. Until this

point, however, it could not have been tuned. In this project, we demonstrated electrical control of coherent coupling via tunnelling of a charge carrier in a quantum dot molecule. Therefore, our work paves the way toward realization of controlled long-range coherent coupling between distant solid state qubits.

Caption

Figure 1: A scheme of a quantum dot molecule device, consisting of a pair of InAs quantum dots (green) vertically separated by 10nm. The first resonant pulse (pulse 1) generates direct and indirect trion complexes in a molecule. The coherence transfer is probed by the optical nonlinearity called four-wave mixing, which is triggered by the second resonant laser pulse (pulse 2).

Figure 1



FURTHER READING



Controlled coherent coupling in a quantum dot molecule revealed by ultrafast four-wave mixing spectroscopy



D. Wigger, J. Schall, M. Deconinck, N. Bart, P. Mrowiński, M. Krzykowski, K. Gawarecki, M. von Helversen, R. Schmidt, L. Bremer, F. Bopp, D. Reuter, A. D. Wieck, S. Rodt, J. Renard, G. Nogues, A. Ludwig, P. Machnikowski, J. J. Finley, S. Reitzenstein & J. Kasprzak

ACS Photonics, **10**, 1504–1511 (2023)



Quantum dot molecule devices with optical control of charge status and electronic control of coupling



F. Bopp, J. Rojas, N. Revenga, H. Riedl, F. Sbresny, K. Boos, T. Simmet, A. Ahmadi, D. Gershoni, J. Kasprzak, A. Ludwig, S. Reitzenstein, A. Wieck, D. Reuter, J. J. Finley

Advanced Quantum Technologies **5**, 2270101 (2022), cover page



Jacek Kasprzak, jacek.kasprzak@neel.cnrs.fr
Daniel Wigger, d.wigger@uni-muenster.de

ON THE HUNT FOR DEFECTS IN β -Ga₂O₃ DEVICES

Ultra-wide bandgap semiconductors, including β -Ga₂O₃, are being used to develop the next generation of electronic devices for high power applications. But what's the point of it in everyday life? Power electronics are everywhere, especially in energy networks. The evolution of our energy production, with more renewable energies, is leading to changes in the way we control the grid: this is where power electronics come in. The most basic device is the Schottky barrier diode, it's often compared to a switch, which allows current to flow in the on state and blocks it in the off state. However, defects inside the device interfere with the switch and prevent it from working properly. We need to identify them in order to remove them.

Beta phase gallium oxide (β -Ga₂O₃) is an emerging ultrawide bandgap semiconductor with promising properties. It has a large bandgap of 4.8 eV, four times larger than that of silicon, it can therefore block much higher voltages. Achievement in growing large-scale (2 inches) and high-quality bulk crystals (semiconductor material) has also motivated the development of high-power devices based on β -Ga₂O₃. Technical developments will allow the availability of potential low-cost and larger substrates within a few years through the melt-grown methods. Although β -Ga₂O₃ has many

advantages, the technological advances of β -Ga₂O₃ are limited by the lack of control over defects and impurities which determine the electronic properties of devices. A better understanding of the origin of deep-level traps is needed.

In our work, we studied two Schottky barrier diodes (Fig. 1) based on β -Ga₂O₃ crystals grown by a method called floating-zone (FZ). Diode 1 was deposited on a mechanically polished substrate and diode 2 on a chemically-mechanically polished substrate. First, we carried out a topographical analysis of the substrates using atomic force microscopy (AFM) to analyze the surface quality. The AFM images (Fig. 2) revealed the presence of scratches on the surface of diode 1 which are expected to be produced by the mechanical polishing. In contrast, on the surface of diode 2 there are much fewer surface defects. The chemical mechanical polishing cycle is more efficient to prepare the substrate surface before the deposition of the metal (Schottky contact).

Then, we used a technique called Deep Level Transient Spectroscopy to investigate the distribution of defects in the bulk and near the surface. Several electron traps have been detected, some of them related to defects usually labeled E1, E2, and E3 in literature for bulk grown by other methods than FZ. We also detected a new defect called E_g, near the surface only in diode 1 (mechanical

polishing) and it is identified as a point defect. We established a link between the polishing cycle and the defect detected near the surface.

We also carried out static analysis to understand the consequences of the surface scratches on the electrical properties of the diode. We extracted different parameters including the barrier height and the ideality factor n . These two parameters help us to understand if we have an ideal switch or not. The barrier height and n indicated the presence of interface states (defects) and inhomogeneities between the metal contact and the semiconductor. E_g and interface defects promote the emission of charges even when the diode is at the off state, the switch is not completely blocking the current as it should do.

Figure 1

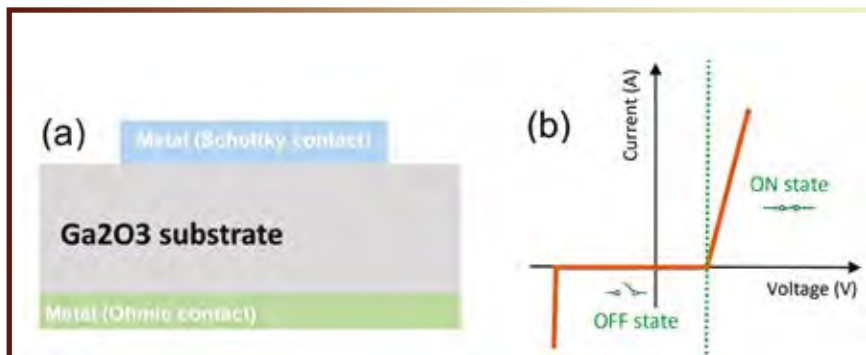
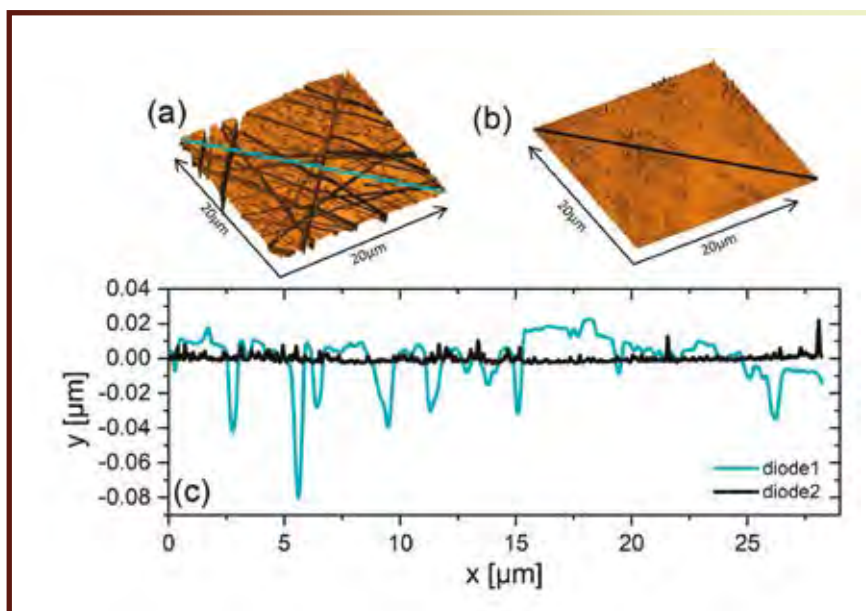


Figure 2



Captions

Figure 1: (a) Sectional view of a vertical Schottky barrier diode: bases on Ga_2O_3 substrate, (b) typical electric characteristic (current vs voltage) with on state (switch on) and off state (switch off).

Figure 2: AFM images of diode 1 (a) and diode 2 (b) showing the presence of scratches on the surfaces of the substrate. (c) Cross profiles of the surface of the two diodes showing the depth and width of the scratches of diode 1 compared to the absence of scratches for diodes 2.

FURTHER READING



Surface defects related to polishing cycle in $\beta\text{-Ga}_2\text{O}_3$ crystals grown by floating zone



C. Perrier, A. Traoré, T. Ito, H. Umezawa, E. Gheeraert & P. Ferrandis

Appl. Phys. Lett. 29 May 2023; 122 (22): 222105. <https://doi.org/10.1063/5.0149969>



Philippe Ferrandis, philippe.ferrandis@neel.cnrs.fr

PhD student:

Coralie Perrier

LOOKING AT MAGNETIC TEXTURES IN 3D

Despite the simplicity of their magnetic structure at the atomic scale, soft ferro-/ferrimagnetic materials can host complex magnetic textures at the mesoscopic scale (from a few nm to a few microns) as a result of the competition between magnetic interactions. Elucidating these textures is necessary to understand their macroscopic properties. Here, we propose an innovative tomographic technique to characterize their magnetic configuration in three dimensions and capturing its vectorial character.

In 2007, Albert Fert obtained the Nobel prize in physics together with Peter Grünberg for the discovery of giant magnetoresistance. A new branch of physics was born, *spintronics*, which exploits both the charge of electrons and their spin, typically in nanoscale components. The physical behavior of these layers strongly depends on magnetization (as a vector) which may or may not be uniform across the considered device. Similarly to nuclear magnetic resonance in medicine, where the imaging provides precious information's on the patient's health, it is crucial to determine the pattern of magnetization (especially as a function of temperature or an applied magnetic field) in order to understand the system's properties.

Laboratory-based magnetic microscopy techniques include (i) magnetic force microscopy

(MFM), (ii) magneto-optical imaging, and (iii) Lorentz microscopy or (iv) electron holography in the Transmission Electron Microscope. These analytical tools are either indirectly sensitive to magnetization (i,iii,iv), or not adapted to three-dimensional systems (ii), or both (i). This illustrates the difficulty to successfully map the magnetization vector field in 3D at the sub-micron scale.

In strong collaboration with the SIMaP laboratory, we use a new promising approach based on Fourier-Transform Holography (FTH), which is well established for 2D magnetic imaging, and we extend its scope to 3D imaging. The experimental demonstration was performed on a $[\text{Fe}(4.5\text{\AA})/\text{Gd}(9.6\text{\AA})]N=600$ multilayer (600 is the number of repetitions of the Fe/Gd bilayer) grown by sputtering in the laboratory. Here Gd (4f of the Mendeleev table) combined with Fe leads to a ferrimagnetic system containing 2 ferromagnetic sub-networks with opposite magnetizations. The field of view is created by a micrometric circular aperture (diameter 5 μm) pierced using focused ion beam through an opaque Au mask on the sample's backside. Then, two 10 $\mu\text{m}\times 80\text{ nm}$ slits are etched through both mask and sample: they serve as holographic references in FTH.

MFM measurements at room temperature and zero field of the multilayer display worm-like magnetic domains (width $\approx 1\text{ }\mu\text{m}$, see Fig. 1). The magnetization is mostly perpendicular to the multilayer, as confirmed by

measuring a magnetic hysteresis loop (average sample magnetization as a function of the magnetic field). Then, **how to detect the 3 components of the magnetization?** The idea is to perform FTH measurements by gradually rotating the sample plane around two orthogonal axes lying in the plane perpendicular to the X-ray beam (each axis is perpendicular to the slit used in the corresponding rotation), and recording small angle coherent diffraction patterns. The latter are modulated by X-ray Resonant Magnetic Scattering. Phase retrieval leads to direct space images proportional to the average projection of the magnetization along the beam axis.

A 3D map of the magnetic moments of the sample at 0 field and room temperature is shown in Fig.2(a), with domain walls (DWs) highlighted in gray. The 3D tomogram reveals that magnetization points mostly out of plane near the surface of the sample but falls in-plane near the substrate, as can be seen in Fig.2(b) for the image in the (YZ) plane. Fine details in the structure of DWs are captured: they consist in Bloch cores (a magnetic "thread" contained in the DW plane) surrounded by Néel caps (moments perpendicular to the DW, closing magnetic flux lines). This first successful step calls for further studies on other interesting textures, possibly under in situ stimuli such as external magnetic fields or electrical currents

Figure 1

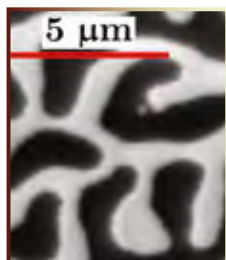
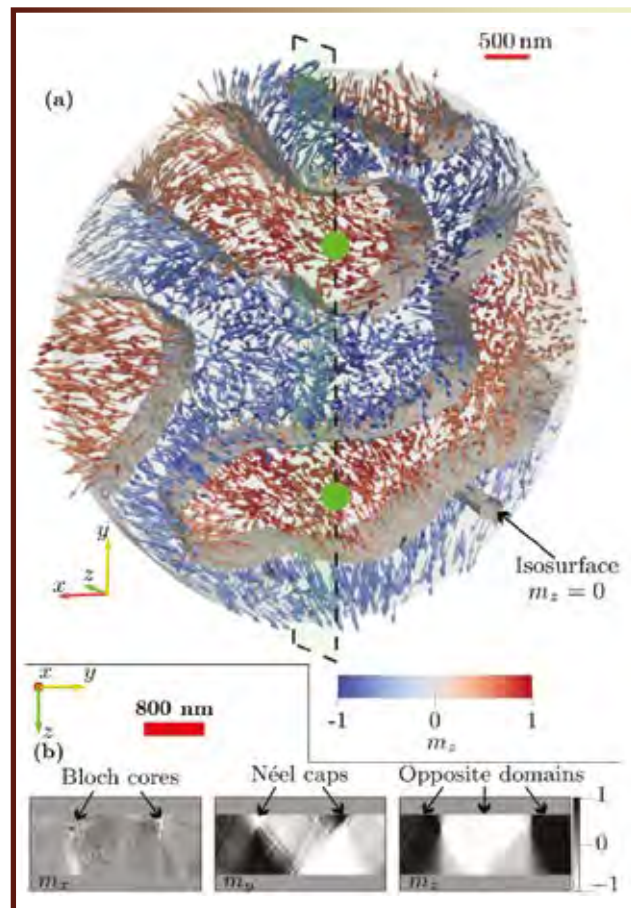


Figure 2



Captions

Figure 1: Magnetic Force Microscopy image of the Fe/Gd multilayer, revealing up and down domains (of opposite contrast).

Figure 2: (a) 3D representation of the Fe/Gd multilayer's magnetic configuration obtained using Fourier transform holography. (b) Slice of the image in the (YZ) plane between the green dots from (a).

FURTHER READING



Three-dimensional tomographic imaging of the magnetization vector field using Fourier transform holography



M. Di Pietro Martínez, A. Wartelle, C. Herrero Martínez, F. Fettar, F. Blondelle, J.-F. Motte, C. Donnelly, L. Turnbull, F. Ogrin, G. van der Laan, H. Popescu, N. Jaouen, F. Yakhou-Harris & G. Beutier

Physical Review B, **107**, 094425 (2023) – Editors' suggestion



Farid Fettar, farid.fettar@neel.cnrs.fr

Alexis Wartelle, alexis.wartelle@neel.cnrs.fr

EXPLORING THE BRAIN'S WONDERS: GRAPHENE MEETS MICROFLUIDICS FOR SMARTER NEUROSCIENCE

The nervous system is incredibly intricate and challenging to study. To better understand how it works, we need innovative tools that simplify the complexity of neural networks and allow us to communicate with neurons. In this research, we use advanced devices called solution-gated graphene field-effect transistors (GFETs) along with a specialized microfluidic platform. This combination enables us to record the electrical activity of neurons in a multimodal and long-lasting manner.

The microfluidic platform has tiny channels that help us define the structure of the neuron network, and the graphene devices offer precise, highly sensitive, and see-through sensing sites. Additionally, calcium imaging shows us how the designed network matures and becomes spontaneously active.

Thanks to the microfluidic circuit, which aligns cells with the sensors efficiently, we achieve an exceptionally high signal-to-noise ratio for detecting single spikes of individual neurons with GFETs. This reveals more information than traditional micro-electrode arrays can capture. By combining graphene sensors and microfluidic circuits, we benefit from the strengths of two cutting-edge technologies for highly

effective sensing of model neural networks.

This new platform is transparent, making it compatible with optogenetic tools or patch clamp to stimulate and further picture the neuron activity. It has the potential to become a versatile lab-on-chip for diagnosing and treating neural disorders in the future, as well as to interface soft or living matter in general.

Despite the high fragility of graphene monolayers, we have successfully integrated highly versatile and high-performance graphene nanodevices with a microfluidic circuit which enables to reconstruct biological neural networks of controlled geometry. Our work demonstrates that arrays of graphene field-effect transistors can be precisely aligned with fluidic microchannels, maintaining both the exceptional electrical performance of GFETs and the high hydrophilicity of the microfluidic circuits for efficient liquid conveyance within narrow channels.

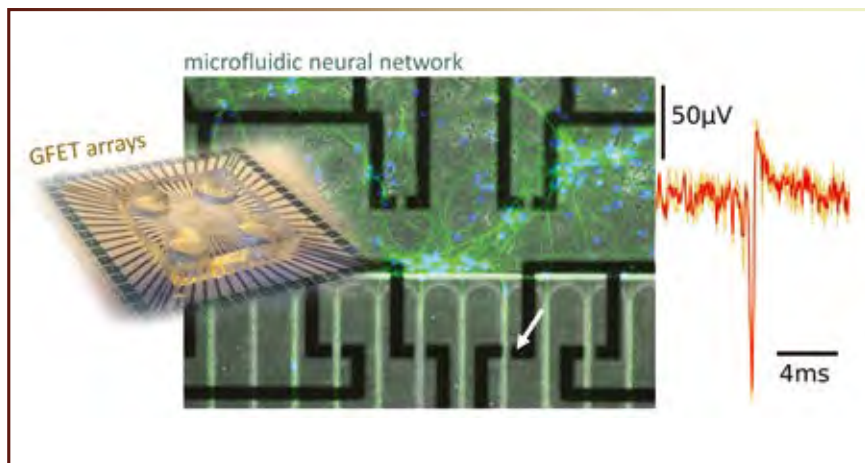
The microfluidic circuit provides an environment conducive to the culture and outgrowth of primary neurons (hippocampal and cortical). Neurons attach efficiently within the spacious chambers, while the microchannels support further growth and selective axon development over the sensing sites. Beyond controlling the to-

pology of the neural network, the combination of GFETs and microfluidic circuits establishes a lasting and localized connection between the cell and electrical devices, optimizing the detection of neural spikes in time.

Our electrical recordings of neural activity, including bursts and single units, showcase the high detection efficiency achieved by combining fluidic microchannels with transparent graphene devices. This efficiency surpasses conventional metallic microelectrodes (MEAs). Notably, our platform allows the clear detection of spontaneous neuronal activity, even at the early stage of culture (DIV4-7), which remain mainly hidden in extracellular recordings. Furthermore, we demonstrate that graphene devices can be utilized in both MEA and FET operations, highlighting the versatility of our sensing platform.

This work represents a promising tool for neuro and biosensing within controlled bio-architectures, serving the needs of both fundamental and applied sciences.

Figure 1



Caption

Figure 1: the figure shows that the combination of graphene transistor arrays with microfluidic circuits (left) enables highly efficient detection and reliable transduction of action potentials (right). Fully transparent microtransistors between the (black) metallic lines allow for both optical and electrical recordings at the sensing site for correlative microscopy. Neurons are confined thanks to the fluidic microchannels that guide in a very accurate and time stable manner the neurites above the graphene transistor channels as highlighted by the arrow.

FURTHER READING



A Multifunctional Hybrid Graphene and Microfluidic Platform to Interface Topological Neuron Networks



V. Dupuit, O. Terral, G. Bres, A. Claudel, B. Fernandez, A. Briançon-Marjollet & C. Delacour

Advanced Functional Materials, 32(49), 2207001 - <https://doi.org/10.1002/adfm.202207001>



Cécile Delacour, cecile.delacour@neel.cnrs.fr

PhD student:

Océane Terral

HYBRID PEROVSKITES: OPPORTUNITIES AND CHALLENGES FOR MEDICAL IMAGING

Due to their unique properties, hybrid perovskites have attracted huge attention as semiconductors for various applications such as photovoltaics, light-emitting diodes, or X-ray detection. Because they can be synthesized at low temperature from solution, they also offer an opportunity for direct integration into optoelectronic devices by crystallization onto readout circuits. Here we present the first attempts at such direct integration, carried out in the scope of the European project Peroxis, revealing in the process specific opportunities and challenges presented by hybrid perovskites for medical imaging.

Hybrid perovskites are often presented as “easily processable from solutions or inks” and regarding their semi-conducting properties to be “quite resilient toward defects”. While this is mainly true, their crystallization presents some peculiarities and many open questions remain regarding the defects impacting their properties. Therefore, making an X-ray medical imager by crystallizing hybrid perovskite on a pixel matrix represents several challenges. To absorb most of the hard X-rays used for medical imaging, perovskite layers should have a thickness close to a millimeter and quite a large

surface area, up to 40x40 cm² for the final sensor. Together these requirements present a unique challenge that can be achieved neither by epitaxy/thin film deposition, nor by bulk single crystal growth. That is why we designed a specific growth system for direct integration of thick polycrystalline layer onto read-out backplanes. It not only took into account the specificities of hybrid perovskite crystallization but was also up scalable to industrial setting. This patented system allowed us to control the hydrodynamics of the solution and thermal geometry in the crystallization chamber and explore a large set of crystallization conditions. While these parameters allowed addressing most of the features expected of the layer (homogeneity, thickness, surface roughness) a fundamental one remained missing: the adhesion of the layer to the backplane.

The lack of adhesion of thick hybrid perovskite to a substrate in solution is a general phenomenon but can it be overcome? By determining the surface energies of our perovskite and the substrates, as well as the surface tensions of the crystallization solutions, we could determine that it is the perovskite/solution interface that is the root cause of the lack of adhesion: the perovskite greatly prefers the solution to the substrate, whatever the crystallization conditions.

Therefore, the perovskite-solution interaction which makes it “easily processable” turns out to be a major drawback here. We have implemented several strategies to overcome that problem: addition of a polymer grid on the substrate to promote adhesion (Fig. 1), indirect coupling of the free-standing layers (bounding to the pixel matrix by a conducting paste).

The various devices realized allowed characterizing their properties and performances in X-ray detection and imaging. These layers allowed demonstrating that they retained the good properties of single crystals (sensitivity higher than commercial imagers, good current stability) but also the less favorable ones (high dark current). Therefore, in order to reach the performances needed for the next generation of medical imagers a better understanding of the correlation between the hybrid perovskite's chemistry and defect structure with its opto-electronic properties is required.

Figure 1

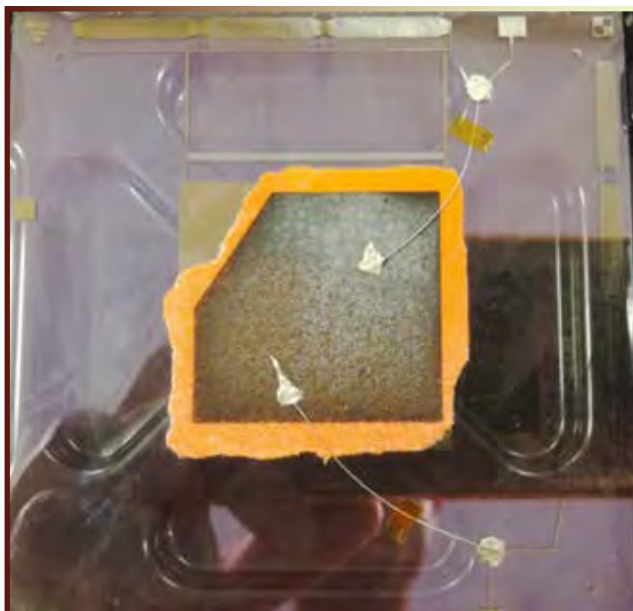


Figure 2



Captions

Figure 1: Device with a 40x40 mm² sensing area made by direct integration of a thick polycrystalline layer of hybrid perovskite onto a pixel matrix. The layer adhesion was achieved thanks to a polymer grid.

Figure 2: X-ray image (bottom) obtained of a lead-letter ghost (top).

FURTHER READING



<https://peroxis-project.eu/>



Julien Zaccaro, Julien.zaccaro@neel.cnrs.fr

Post-Doc

Thibault LEMERCIER

AMORPHOUS TOPOLOGICAL STATES: A DISORDERED PLAYGROUND FOR NEW PHENOMENA

Modern condensed matter physics cannot be understood without topology. Topological insulators are materials discovered in the last decades with properties between metals and insulators. Topological insulators have an insulating interior, but their surfaces or edges conduct. These conducting states exist due to global, topological, properties of the electron's wave-function. Hence, they are robust and cannot be removed by simply introducing impurities or disordering the material. Understanding when and why such robustness emerges is a fundamental problem in condensed matter. Solving this problem may allow to associate useful technological properties to such robust behaviour, and be a stepping stone for quantum computing architectures.

Topological phases of matter are ubiquitous in crystals, but less is known about their existence in non-crystalline solids, like amorphous solids that lack long-range order. Technology built of amorphous solids is ubiquitous and affordable, as they are easier to grow than high-quality crystals. Our group specialises in finding theoretical models and tools to understand topological phases in non-crystalline matter, which we currently lack. We have recently reviewed the status of the field (see "further reading"). This year our group has developed

tools that identify non-crystalline topological insulators and we have found topological phases that occur because the system is non-crystalline.

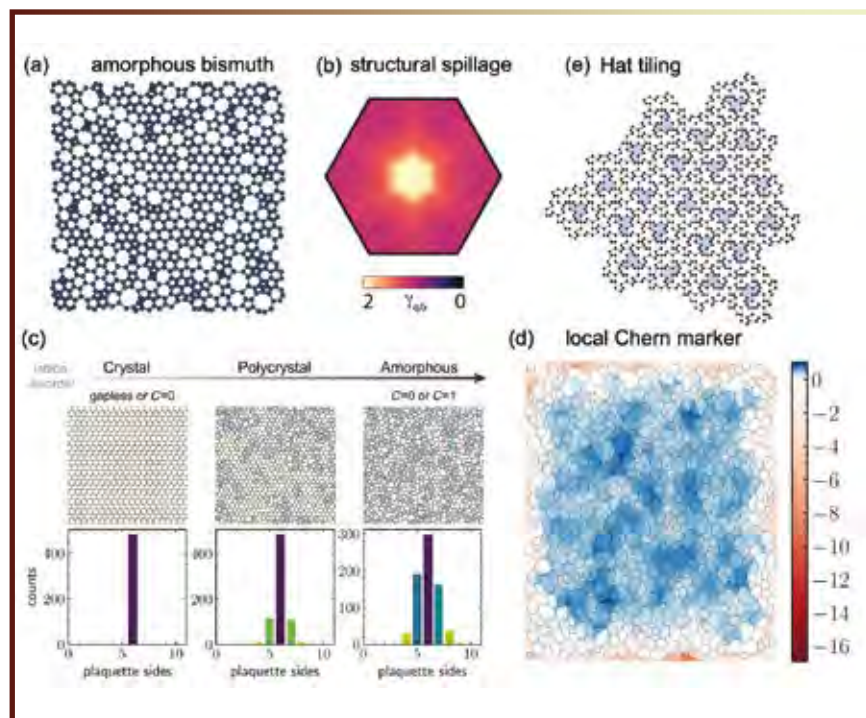
We have proposed a simple tool to know if a non-crystalline system is topological or not by comparing its wave function with a known crystal. We called this tool structural spillage. In Fig. 1 (a) we show a model of 2D amorphous bismuth, and its *structural spillage* in (b). To find if (a) is topological we compared the wave-functions of a bismuth 2D crystal without spin-orbit coupling, known to be topologically trivial, to those of (a). The structural spillage, shown in (b), shows a bright peak at the Brillouin zone center of the original crystal, indicating that the wave-functions differ at certain momenta. This peak is an indicator of topology because it measures the difference between band inversion between the amorphous and crystalline solid.

We have also proposed topological phases of matter that exist only because the material is amorphous. In a collaboration with C. Repellin at LPMMC, we found an exotic type of topological phase, known as a chiral spin-liquid, induced by amorphization. It emerges in systems that have spins with three nearest neighbours and strong spin-spin frustration. In spin-liquids, the frustration prevents the spins to order even at zero temperature.

We found that as a honeycomb lattice filled with spins becomes more and more disordered, see Fig. 1 (c), an exotic state emerges. It has no spin order but features a collective excitation that carries heat unidirectionally along the edge, called a chiral Majorana edge mode. The robustness of such an excitation increases as we increase the disorder! , see Fig. 1(d). This property could help to realise exotic topological phases in the laboratory by growing known spin-liquid candidate materials as amorphous solids.

In the future our goal is to use our tools to find more exotic phases, but also real materials in which they can be realised. Moreover, we are branching out towards other non-crystalline materials, including quasicrystals. We have shown that a newly discovered quasicrystalline lattice, the Hat tiling shown in Fig. 1 (e), can host electronic properties in between crystals and quasicrystals, a previously unseen phenomenon. In short, we are excited to see what surprises the interplay between non-crystallinity and topology can bring in the near future.









Figure 1



Caption

Figure 1: Amorphous 2D bismuth model. (b) Structural spillage obtained by comparing 2D amorphous and crystal-line bismuth, with and without spin-orbit coupling, respectively. The central peak in the Brillouin zone indicates band inversion, a known indication of topology. (c) Amorphization of a honeycomb lattice. (d) The color represents the Local Chern marker, an observable related to the local thermal Hall conductivity. Its quantisation to +1 in the bulk of the system indicates a topological chiral spin-liquid phase. (e) The Hat tiling, a newly discovered quasicrystalline lattice. It is composed of tiles called hats and their mirror image, highlighted in blue.

FURTHER READING

-  [1] Amorphous topological matter: theory and experiment
 P. Corbae, J. D. Hannukainen, Q. Marsal, D. Muñoz-Segovia, A. G. Grushin
European Physics Letters 142, 16001 (2023)
-  [2] Structural spillage: an efficient method to identify non-crystalline topological materials
 D. Muñoz-Segovia, P. Corbae, D. Varjas, F. Hellman, S. M. Griffin, A. G. Grushin
Phys. Rev. Research 5, L042011 (2023)
-  [3] Amorphous and polycrystalline routes towards a chiral spin liquid
 A. G. Grushin, C. Repellin
Phys. Rev. Lett. 130, 186702 (2023)
-  [4] Physical properties of the Hat aperiodic monotile: Graphene-like features, chirality and zero-modes
 J. Schirmann, S. Franca, F. Flicker, A. G. Grushin
arXiv: 2307.11054, Phys. Rev. Lett. (in press, 2024)

✉ Adolfo G. Grushin, adolfo.grushin@neel.cnrs.fr

PhD student:

Justin Schirmann

Post-Doc

Selma Franca

EFFICIENT, NON-TOXIC MICROWATT THERMOELECTRIC MICROGENERATORS

Thermoelectricity relies on the principle of direct conversion of heat into electricity, or vice versa. Many materials with interesting thermoelectric properties were discovered in the 1950s and 1960s. These include the bismuth telluride (Bi_2Te_3) used in commercial Peltier modules, and the silicon-germanium (SiGe) alloys used to power space probes in radioisotope thermoelectric generators. In collaboration with colleagues from Institut de Chimie et des Matériaux Paris-Est, we have optimized the thermoelectrical properties of cost-effective and non-toxic Fe-V-Al thin films and developed a microgenerator able to generate 5 μW power output under a temperature difference of 134K.

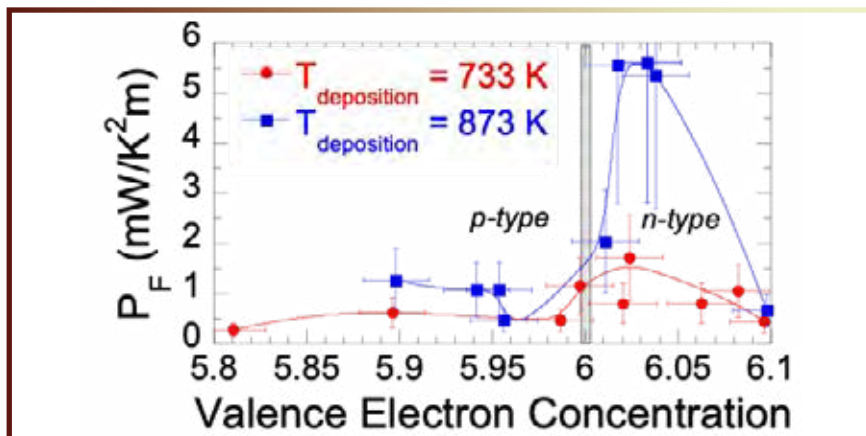
A significant milestone was achieved through the successful enhancement of the P_F power factor which is one of the main parameters characterizing performance of thermoelectrics. This physical quantity represents the electronic transport properties for thermoelectric materials ($P_F = S^2\sigma$ with S the Seebeck coefficient and σ the electrical conductivity). We observed that optimizing the deposition conditions, specifically by working with temperatures close to 873 K and fine-tuning the film's composition using a DC

magnetron co-sputtering process can significantly improve the power factor P_F . In fact, an unprecedented power factor of up to 5.6 $\text{mW/K}^2\text{m}$ for n-type films deposited at 873 K, setting a new record for Fe_2VAl thermoelectric thin films has been obtained. Magnetron sputtering deposition was achieved using ternary Fe_2VAl as the principal target elaborated by induction melting. A secondary target of V or Al was also used during deposition to finely tune the film composition. A detailed study has shown that the Seebeck effect and the power factor are strongly dependent on the valence electron concentration linked to the composition of the thin film (Fig. 1).

After a work of thermoelectric properties optimization for n- and p-type Fe_2VAl thin films, microgenerators consisting of five n-p couples deposited on Al_2O_3 substrate were fabricated and tested (Fig. 2). These thermoelectric microgenerators have demonstrated their remarkable potential in practical energy harvesting. They have achieved microwatt power output, with a maximum electrical power output of nearly 5 μW measured at a temperature difference of 134 K. The resulting maximum power density is close to 60 mW/cm^2 , placing these microdevices among the highest-performing in their class.

Intriguingly, the resilience of these microgenerators to contact resistance sets them apart from other thermoelectric materials like Bi_2Te_3 or PEDOT (polymer composite). These devices, assembled with junctions between Fe-V-Al and aluminum electrodes, exhibit minimal sensitivity to contact resistance, further bolstering their potential for integration into the Internet of Things (IoT) domain. This feature holds the promise of powering autonomous sensors with unmatched efficiency, making them well-suited for the IoT's growing demand for sustainable and reliable energy sources.

Figure 1

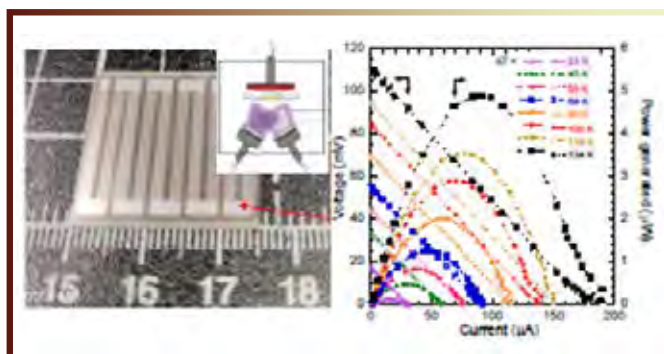


Captions

Figure 1: Power factor vs valence electron concentration for Fe-V-Al thin films deposited by a DC magnetron co-sputtering process at 733 K (in red) and 873 K (in blue)

Figure 2: Microwatt power output obtained in thermoelectric microgenerators based on cost-effective and non-toxic Fe-V-Al thin films deposited by a DC magnetron co-sputtering process.

Figure 2



FURTHER READING



Improved Power Factor in Self-Substituted Fe₂VAl Thermoelectric Thin Films Prepared by Co-sputtering



D. Bourgault, H. Hajoum, S. Pairis, O. Leynaud, R. Haettel, J. F. Motte, O. Rouleau, E. Alleno.

ACS Appl. Energy. Mat. 2023 6, 3, 1526–1532 <https://doi.org/10.1021/acsaem.2c03405>



Unlocking Microwatt Power: Enhanced Performance of Fe-V-Al Thin Films in Thermoelectric Microgenerators



D. Bourgault, H. Hajoum, R. Haettel, E. Alleno, J. Mater.

Chem. A, 2023, 11, 19556 – 19565. <https://doi.org/10.1039/D3TA04080A>



Daniel Bourgault, daniel.bourgault@neel.cnrs.fr

Richard Haettel, richard.haettel@neel.cnrs.fr

Supported by Institut Néel since 2015, the project to acquire a state-of-the-art Transmission Electron Microscope (TEM) was born of the joint desire of Institut Néel and Constellium to gather their respective expertise in the development of advanced materials.

From 2019, complementary skills and converging needs between Constellium and Institut Néel, two entities in the Grenoble area, have triggered a collaborative approach focused on the accurate structural study of innovative materials.

The Transmission Electron Microscope is a powerful instrument for probing matter down to the atomic level. The development of new materials to meet socio-economic challenges, in industrial sectors as varied as the automotive, aeronautical and packaging industries, relies on knowledge of their internal microstructure, which is essential for improving their physical properties (mechanical, optical, electrical, etc.). The fields of application are varied: in addition to metallurgy, they include pharmaceuticals, soil decontamination, organic photovoltaics, micro/nanoelectronics, coatings, batteries, nanotechnologies and photonics.

The features of the JEOL NEOARM microscope are :

- A fully-equipped instrument that allows the sample to benefit

from the complementarity of cutting-edge techniques in a single device: 4 acceleration voltages, 3 state-of-the-art cameras, including one with direct detection via the ERC, 2 spectrometers, 1 bi-prism, 1 SAAF detector.

- A state-of-the-art TEM in a physicists' environment, to promote synergy between the study of physical properties and very high-level atomic scale characterization.

- The high level of Institut Néel's expertise for new technical developments (e.g. in situ cryogenic experiments).

- A very high-quality installation, with low mechanical and electromagnetic noise, regulated temperature and hygrometry, remote workstation, allowing ultimate resolution.

The TEM facility JEOL NEOARM at CNRS Institut Néel was co-financed by the European Union under the European Regional Development Fund (*ERDF*, contract n° RA0023813).

Figure 1



Caption

Figure 1: JEOL NEOARM Transmission Electron Microscope.



Project team

Stéphanie Kodjikian,
Holger Klein,
Martien den Hertog,
Christophe Lepoittevin,
Etienne Bustarret



Stéphanie Kodjikian,
stephanie.kodjikian@neel.cnrs.fr



HIGHLIGHTS N°17

Institut Néel - CNRS
25, avenue des Martyrs - BP166
38042 Grenoble Cedex 9
France

